THREE-DIMENSIONAL SEEPAGE ANALYSIS OF A COAL REFUSE PILE RECLAMATION[1]

Iuri Lira Santos[2], Leslie C. Hopkinson, John D. Quaranta, and Paul F. Ziemkiewicz

Abstract. A coal refuse pile located in Greenbrier County, West Virginia was studied to restrict generation of acid mine drainage through the use of a cap and cover system. This paper presents results of a finite element method seepage analysis on a proposed reclamation design. The proposed reclamation incorporates a cap and cover system with a 0.3-m thick surface vegetation cap layer over a 0.6-m thick low permeability layer. The low permeability layer is directly above the coal refuse. Unsaturated soil mechanics was utilized, adopting the Fredlund and Xing equation for soil-water characteristic curve (SWCC) estimation. SWCC fitting parameters were calculated using the Zapata and the Hernandez estimation techniques. Different precipitation events were used to evaluate seepage throughout the reclamation area and assess the effectiveness of the cap and cover system. A steep area (>4H:1V) and a flat area were considered. The water balance analysis showed a 50% to 88% reduction in water volume at the coal refuse layer and a reduction in the time for the refuse to return to initial water content due to the cap and cover system implementation. Moisture detainment was observed in the growth layer and is important for supporting vegetation persistence.

Additional Key Words: Water balance covers, finite element modeling, unsaturated soil mechanics

---

[1] Paper presented at the 2019 National Meeting of the American Society of Mining and Reclamation, Big Sky, MT, ***The Land of Reclamation Pioneers*** June 3 - 7, 2019. R.I. Barnhisel (Ed.) Published by ASMR, 1305 Weathervane, Champaign, IL 61821.

[2.] Iuri Lira Santos is a Graduate Research Assistant, Civil and Environmental Engineering, West Virginia University, Morgantown, WV 26506; Leslie C. Hopkinson is an Associate Professor of Civil and Environmental Engineering, West Virginia University, Morgantown, WV 26506; and John D. Quaranta is an Associate Professor of Civil and Environmental Engineering, West Virginia University, Morgantown, WV 26506; Paul F. Ziemkiewicz is Director of the West Virginia Water Research Institute, West Virginia University, Morgantown, WV 26506.

DOI: http://dx.doi.org/10.21000/JASMR20040044

Introduction

Landfills are designed and constructed to regulate the flow of gases and liquid into the subsurface to restrict the release of contaminants to the environment. This is commonly accomplished by managing water penetration into the landfill. Cap and cover systems (also known as alternative covers, store and release covers, or water balance covers) can be designed in several configurations depending on its final purpose, availability of materials, and cost of execution. Conventional covers utilize a low permeability layer above contaminated material to minimize water movement. Typical configurations include a soil cover (e.g., growth layer), a low conductivity soil layer or a geosynthetic clay liner, a composite, or a combination (Albright et al., 2010).

Cap and cover systems are utilized for isolation to control environmental concerns. For example, cap and cover systems are used to seal radioactive waste (Daniel, 1983), for landfills (Nyhan et al., 1990; Warren et al., 1996), and to control acid mine drainage (AMD) in mine refuse reclamation (Kim and Benson, 2004; Rowe and Hosney, 2013). The application of a cap and cover system to control AMD is the focus of this research. Control of environment damage caused by AMD is normally conducted using two approaches: i) "controlling the source" by reducing the generation of AMD, or ii) "mitigation measure" in which the produced AMD is amended for disposal (Johnson and Hallberg, 2005). Cap and cover systems control the source by reducing the amount of AMD produced.

Cap and cover systems often include a vegetation growth layer to create resistive forces against erosion, protect from freeze-thaw effects, reduce the rain splash effect, reduce runoff velocity, and reduce soil particle movement (Gray and Sotir, 1995). Vegetation aids in the maintenance of the water balance, consuming water from the topsoil layer, thus reducing infiltration and producing a better aesthetical appearance to the reclamation (Peppas et al., 2000).

Depending on the soil media being utilized as a vegetation substrate, an additional nutrient supply may be needed for vegetation establishment. Biosolids have been proven as an effective nutrient supply to be used in surface mine reclamation. Research on different biosolids utilized in reclamation of mine refuse piles indicated lumber mill waste, sewage sludge, and short paper fiber (SPF) as three potential materials as a component of manufactured soil utilized in the growth layer of a cap and cover system (Daniels and Zipper, 2010; Cyphers et al., 2018).

Schuman and Sedbrook (1984) identified lumber mill waste as an appropriate reclamation alternative for bentonite mine spoils, and Lunt (1955) verified an increase in soil organic matter and pH moderation when lumber mill waste was utilized in coarse soils. Skousen and Clinger (1993) monitored three years of a municipal wastewater sewage sludge application in a reclaimed surface mine in West Virginia. Four different concentrations were applied to the site, resulting in an increase in grass biomass, organic carbon; however, no relevant change in pH was observed. Seaker and Sopper (1983) also performed monitoring over a mine refuse site with municipal sewage application (rates of 80 Mg/ha and 108 Mg/ha) over a five-year period. They verified enhancement of soil conditions for vegetation growth over the mine refuse with no negative effects presented during the research period.

This research addresses the potential use of SPF as part of a manufactured soil in the growth layer of a cap and cover system. SPF is a byproduct of paper production and has a high organic content. For example, Ziadi et al. (2013) reported the following ranges of paper biosolid nutrient contents: 294-438 g/kg, 4.5-231.5 g/kg, 1-5.8 g/kg, and 0.5-3.3 g/kg for total carbon, total nitrogen, total phosphorus, and total potassium, respectively. Several studies have found benefits of implementing SPF as a soil amendment. Camberato et al. (2006) identified an increase in organic matter and water holding capacity and a reduction in erosion due to soil aggregation. Cyphers et al. (2018) evaluated a coarse coal refuse (CCR) and SPF blend for vegetation growth, mixed in different volumetric proportions. Results showed an increase of up to 70% in ground coverage by vegetation per area studied. Carpenter and Fernandez (2000) verified different manufactured topsoil amended with paper fibers were successful in obtaining N mineralization and resulted in improvement in cation exchange capacity and P concentration.

Cap and cover systems are normally designed by applying unsaturated soil mechanics theory seepage analysis (Benson and Bareither, 2012). Different soils will present different affinities for water, which is described as matric soil suction. Fredlund and Xing (1994) performed regressions of experimental testing results that culminated in equations describing matric suction as a function of water content (equations 1 and 2), resulting in the soil-water characteristic curve (SWCC):

$$\theta(\Psi, a, n, m) = C(\Psi)\frac{\theta_s}{\{\ln[e+(\Psi/a)^n]\}^m} \quad \textbf{(1)}$$

$$C(\Psi) = \frac{-\ln(1+\Psi/\psi_r)}{\ln[1+(1{,}000{,}000/\psi_r)]} + 1 \quad \textbf{(2)}$$

Where: θ = Volumetric water content,

θ_s = Saturated volumetric water content,

$C(\Psi)$ = Correction factor for suction = 10^6 kPa at zero water content,

a = Parameter function of the air entry value of the soil,

n = Parameter function of the rate of water extraction of the soil,

m = Parameter function of the residual water content (θ_r),

Ψ = Soil water suction, and

Ψ_r = Suction corresponding to the residual water content.

When a coarse soil is evaluated, high values of air entry parameters are found in the curve, resulting in a rapid fall of the slope followed by a long tail. When evaluating finer materials, the water affinity is higher, thus high values of matric suction are observed for lower water contents when compared to coarse soils. Lu and Likos (2014) describe water affinity presenting the capillarity effect where in fine soils the water tension is higher raising the waterfront higher than in coarse materials.

Along with other parameters, the hydraulic conductivity can be generated from the SWCC. Fredlund et al. (1994) established a model for the estimation of hydraulic conductivity integrating the SWCC parameters along the volumetric water content range reaching the saturated stage at air entry value (equation 3):

$$k = k_{sat}\left\{\frac{\int_{\ln\Psi}^{b}(\theta(e^y)-\theta(\Psi)/e^y)\theta' e^y\,dy}{\int_{\ln\Psi_{aev}}^{b}(\theta(e^y)-\theta_s/e^y)\theta' e^y\,dy}\right\} \quad \textbf{(3)}$$

Where: k_{sat} = Hydraulic conductivity at saturated conditions,

y = Variable function of the water content,

Ψ_{aev} = Air entry value,

θ' =Correction factor for tortuosity,

b = Suction corresponding to residual water content.

The overall objective of this work was to simulate the performance of a cap and cover system designed for controlling AMD infiltration in a coal refuse pile in West Virginia. The cap and cover system were composed of a growth layer and low permeability layer; the growth layer utilizes *in-situ* material combined with SPF to limit the need for off-site material. The cap and cover system performance were tested with multiple precipitation events for a steep (slopes greater than 1V:4H) and a flat portion of a developed reclamation plan. Two designs were considered, both with the same base refuse layer: one with the cap and cover system and one without. The intent was to compare the volumetric water difference (VWD) at the refuse due to the system implementation. A three-dimensional finite element seepage model of the proposed reclamation plan for the coal refuse site was performed. The model was executed in a transient analysis utilizing unsaturated soil mechanics.

Background: Cap and cover system design

The cap and cover system studied in this work was designed as part of a reclamation plan for a coarse coal refuse in Greenbrier County, WV, as described by Hopkinson et al. (2017). The intent was to control AMD by promoting infiltration into and evapotranspiration out of the growth layer and to minimize infiltration into the refuse pile (Skousen et al., 2019). Figure 1 illustrates the cap and cover system design; it is composed of two layers configured above the *in-situ* mine refuse base layer: a low permeability layer and a growth layer.

a) b)

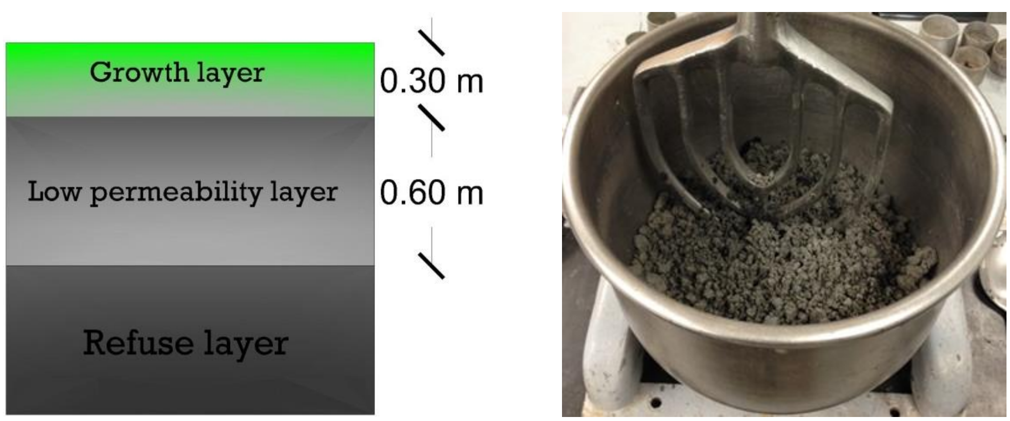

Figure 1. a) Cap and cover system layering and b) growth layer blend appearance.

The low permeability layer was designed as a 0.60-m compacted refuse layer consisting of the refuse material that was regraded to the specified surface elevation contours. The 0.30-m thick growth layer was composed of a combination of SPF and *in-situ* refuse material with a volumetric proportion of 60% refuse material to 40% MGro™ (SPF) (Figure 1).

Methods

Site Description

The pile consists of coarse coal refuse, a pyritic shale which is producing AMD. The site was abandoned in 1999 and continues to produce AMD. The refuse pile (19.27 ha) is characterized by minimal vegetation coverage. The effluent is being treated with conventional settlement ponds for pH stabilization and metal removal. The site is in a mountaintop, and the unique water recharge is precipitation. The site exhibits gullies, distributed surface water channeling, and high subsurface infiltration. A geomorphic reclamation plan mitigating these issues was designed for this site (i.e., Hopkinson et al. 2017) and served as the base design for this paper. Ward (2001) identified the site yearly treatment cost surpasses $220,000. Santos (2017) stated that for the year of 2015 the AMD treatment for the site cost totaled $173,324, including chemicals, labor, and site maintenance; and, the budget for executing a conventional reclamation is $2,288,385 versus $2,959,494 for the geomorphic reclamation.

Soil Characteristics

Soil characteristics of the primary components of the cap and cover system were defined by Stevens (2016) and Tolikonda (2010) (Table 1). The saturated hydraulic conductivity of the growth layer was three orders of magnitude (cm/s) greater than the low permeability layer. Porosity ranged from 0.18 for the low permeability layer to 0.52 for the growth layer. All soil layers were considered three dimensionally isotropic. The unsaturated hydraulic conductivity was calculated by the Fredlund and Xing (1994) estimation utilizing the saturated hydraulic conductivity values presented herein.

Table 1. Soil hydraulic and strength properties (Data retrieved from: Tolikonda, 2010; Stevens, 2016)

Material	Saturated Hydraulic Conductivity (cm/s)	Porosity	Specific Gravity
Fill	4×10^{-4}	0.45	2.65
Low permeability layer	2×10^{-6}	0.18	2.31
Growth layer	1×10^{-3}	0.52	2.00

The unsaturated properties for the soils used in the modeling were assigned by characterizing the soil-water characteristic curves. Two grain size distribution curves are illustrated in Figure 2 and are used as the base for the Fredlund and Xing (1994) SWCC equation parameters. Grain size distribution of the growth layer is similar to the *in-situ* soil, as reported by Stevens (2016). The SWCC fitting parameters are considered equivalent since they are calculated based on the GSD. Two different methods were utilized for the calculation of the SWCC parameters according to their suitability: 1) Zapata (1999) was utilized for the *in situ* soil (fill and growth), and 2) Hernandez (2011) was used for the low permeability layer.

Zapata (1999) defines the SWCC parameters based on grain size distribution and plasticity of the material, when applicable, and no hysteresis is considered. The method correlates the diameter corresponding to the 60% finer fraction in the particle size distribution (D_{60}) to the fitting parameters of the Fredlund and Xing (1994) SWCC (equations 1-2), by equations 4 to 6:

$$a_{fz} = 0.8627(D_{60})^{-0.751} \quad \textbf{(4)}$$

$$m_{fz} = 0.1772(\ln(D_{60})) + 0.7734 \quad \textbf{(5)}$$

$$\Psi_{rfz} = a_f(\frac{1}{D_{60}+9.7e^{-4}}) \quad \textbf{(6)}$$

where fitting constant n_{fz} is 7.5.

The subscripts "*f*" denotes fitting parameter into the Fredlund and Xing (1994) equation, and "*z*" denote that the fitting parameters were calculated by the Zapata (1999) estimation.

The low permeability layer SWCC estimation was performed by using the Hernandez (2011) model (equations 7 to 9) which is more suitable for soils with a higher fines content. This method utilized the diameter corresponding to the 10% finer fraction in the particle size distribution (D_{10}) as the soil gradation parameter input.

$$a_{fh} = -967.21D_{10} + 218.37D_{10} - 2.7 \quad \textbf{(7)}$$

$$n_{fh} = 10(-0.0075a_f + 0.1133a_f - 0.3577a_f + 0.3061) \quad \textbf{(8)}$$

$$m_{fh} = 0.0058a_f - 0.0933a_f + 0.4069a_f + 0.3481 \quad \textbf{(9)}$$

where fitting constant Ψ_{rfh} is 100.

The subscripts "*f*" denotes fitting parameter into the Fredlund and Xing (1994) equation, and "*h*" denote that the fitting parameters were calculated by the Hernandez (2011) estimation.

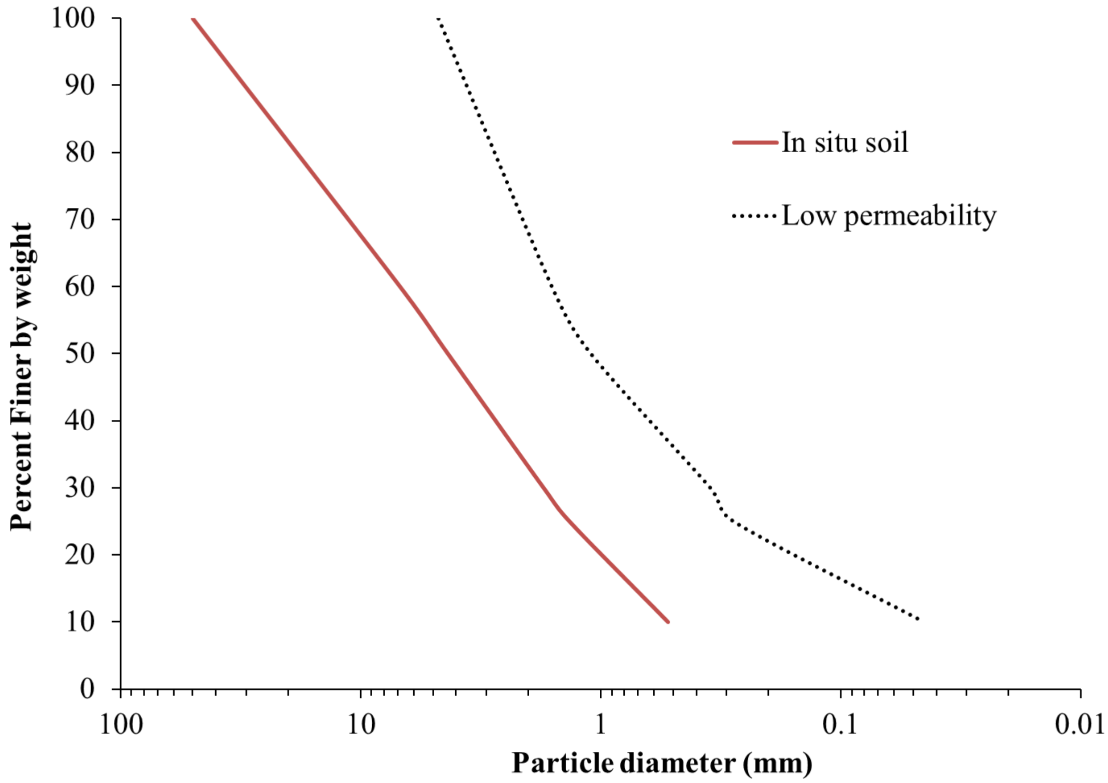

Figure 2. Grain size distribution (GSD) for the modeled soils Data retrieved from: Tolikonda, 2010; Stevens, 2016).

In this work, the Zapata (1999) estimation for the *in-situ* soil was calculated with a D_{60} of 1.0 mm as it is the upper boundary for this model. The Hernandez (2011) estimation was calculated with a D_{10} of 0.07 mm. The fitting parameters a_{fz}, n_{fz}, m_{fz}, and Ψ_{rfz} were calculated to be 0.86, 0.77, 7.5 and 0.73, respectively, for both the *in situ* and growth soils. The low permeability layer fitting parameters a_{fh}, n_{fh}, m_{fh}, and Ψ_{rh} were calculated to be 5.17, 2.81, 0.75 and 100. Fitting parameters were applied to equations 1 and 2 for SWCC generation (Figure 3).

With SWCC defined for each soil, the Fredlund et al. (1994) method for unsaturated hydraulic conductivity can be applied (Figure 4). Unsaturated behavior mirrors the SWCC and reflects the saturated hydraulic conductivity at the air entry value.

Simulation description

The four events selected for precipitation for each model were a 24-hour duration rainstorm with 1-, 5-, 25-, and 100-yr recurrence interval, corresponding to a 59 mm, 82 mm, 112 mm, and 139 mm rainfall depth, respectively (NOAA, 2018). The model used a daily time step starting day 0, and the precipitation events were applied at day 1 for an initial volumetric water content before precipitation. Evapotranspiration was applied at a constant rate using the modified Wilson-Penman (Wilson et al., 1994) method. The air temperature, humidity, and solar radiation were set as 20^{o}C, 70%, and 20 Mj/m^2/day, respectively (NOAA, 2018; NREL, 2019). These values remained constant among all simulations. Reflection coefficient, sunshine ratio, and wind speed were set as constant values of 0.05, 0.65, and 1 m/s, respectively, with no crust formation or vegetation. These values were selected for simulation for the months of May and June. A low reflection rate was selected for the material due to its black color.

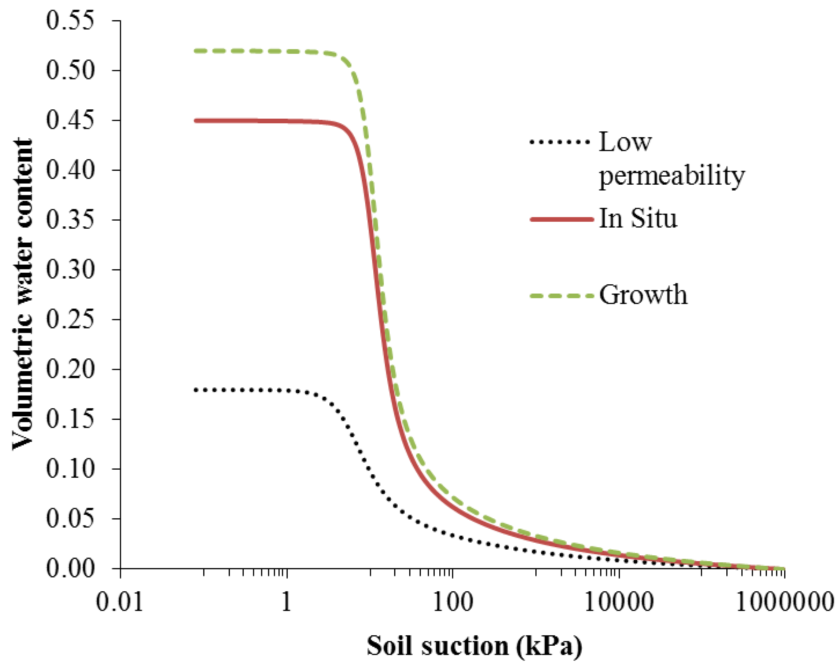

Figure 3. Estimated SWCCs for the modeled soils.

Model Geometry

Seepage modeling in this research was performed using the SoilVision® software with the SVFlux® module. The cap and cover system layers were created utilizing the geometry from the final watershed design of the site reclamation project (Figure 5). Two models were created: 1) a steep slope model (slopes greater than 1:4 (14.04^{o})) and 2) a flat model (slopes < 1:4). Site accounting for steep slopes was performed using Carlson® Civil suite 2016 identifying 11.82 hectares of the 19.27 hectares as flat slopes with average slope angle of 6.3°, and 7.45 hectares as steep slopes with slopes averaging at or above 20°.

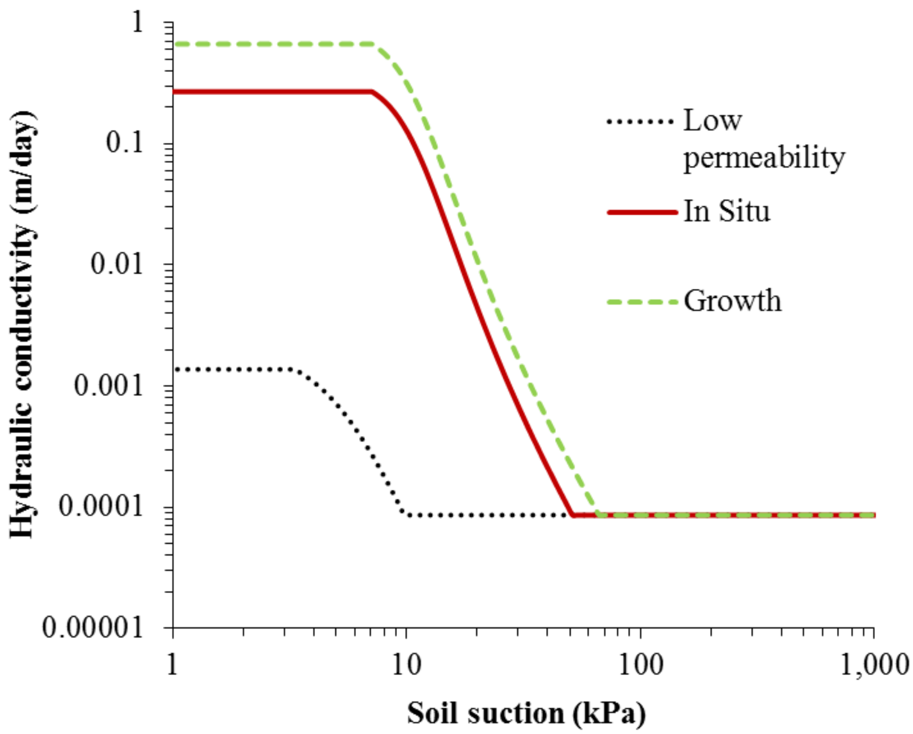

Figure 4. Hydraulic conductivity functions of the modeled soils.

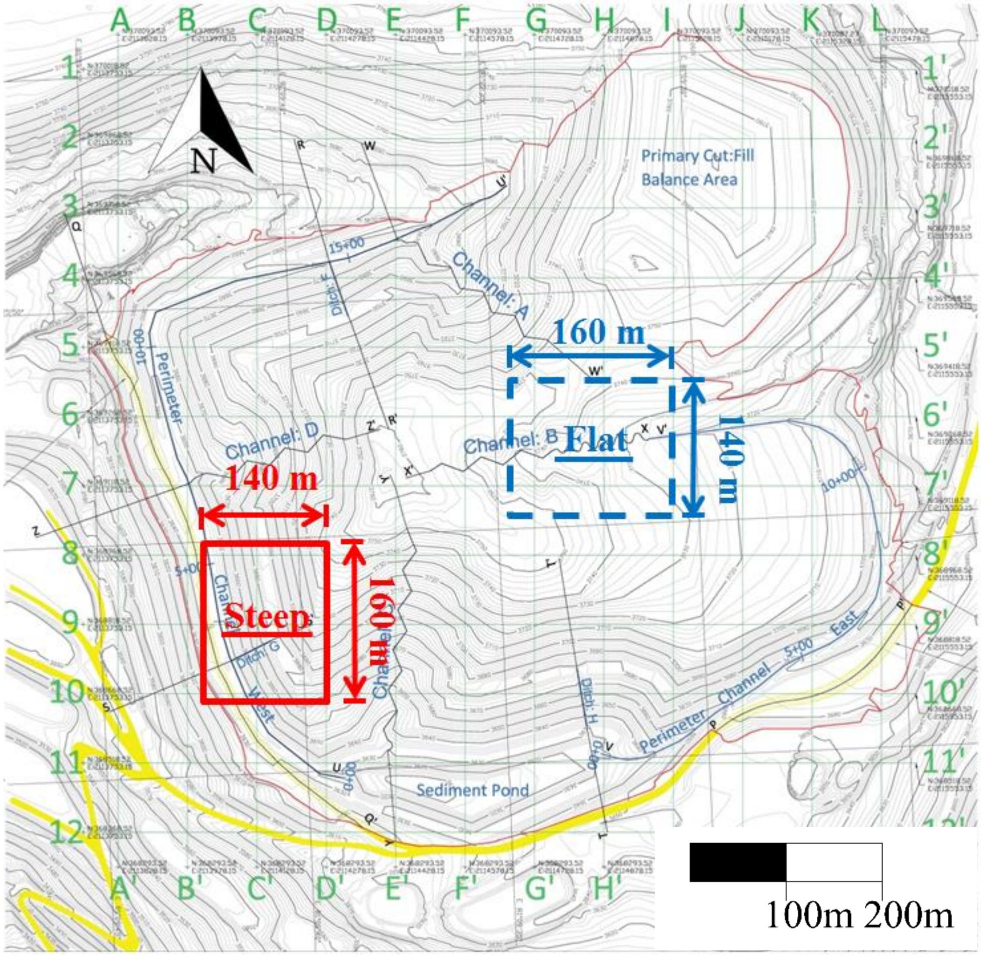

Figure 5. Modeling region's steep and flat locations on the project. Adapted from (Hopkinson, et al., 2017).

The surface grid was composed of 20-m side squares resulting in a projected area of 22,400 m^2 for both the steep and flat model (Fig. 5). A water table was set 1 m vertical distance above the bottom of the refuse layer. Representation of the steep model in the SVFlux® software environment is presented in

Figure 6. The flat modeling area (Figure 7) contains the beginning of a drainage channel and that discharges in the east channel of the watershed design. The coordinates of the corners provide visualization of the relief of the geometry. For modeling purposes, coordinates were transposed to be relative to the model (having a corner at (0, 0, 0) for both steep and flat). Surface grids are delineated in the dashed blue lines and the model elements in the dashed black line.

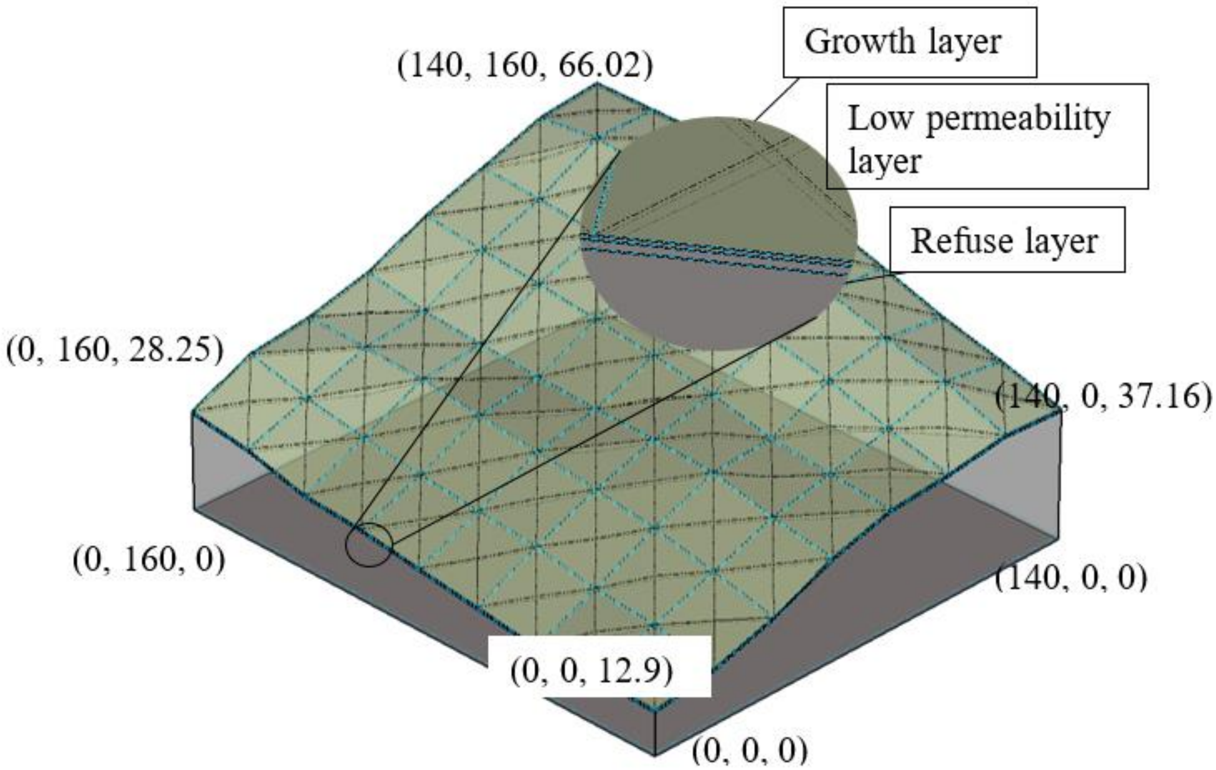

Figure 6. Steep model representation; local coordinates in meters. Inset demonstrate layers in the model

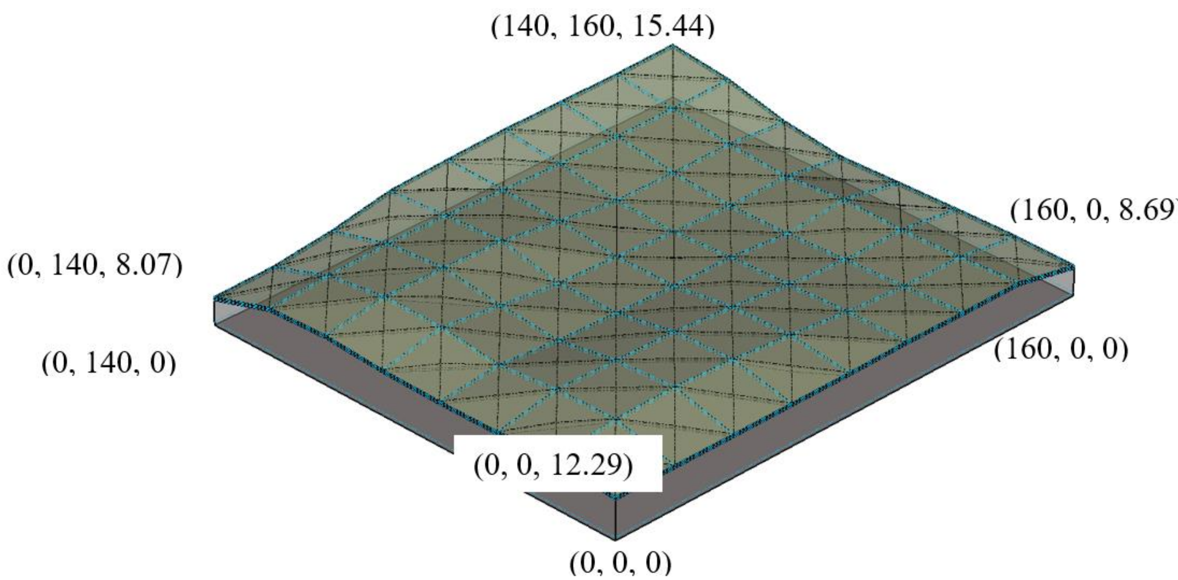

Figure 7. Flat model representation; local coordinates in meters.

Results and Discussion

Refuse layer water content

The volumetric seepage analysis focused on identifying the reduction in water volume at the refuse layer. Effectiveness of the reclamation is evaluated by comparing the maximum volumetric water difference (VWD) in the refuse presented by the steep and flat models with and without the cover.

The first result observed is the time difference for the model to return to the initial volumetric water balance due to evapotranspiration and seepage (Table 2). For the flat slope model, effectiveness of the low permeability layer presents more evidence when evaluating the water movement velocity. Reduction of runoff by water infiltrating in the growth layer creates high gradients for water seepage, accumulating more water in the low permeability layer pores. In the uncovered model, seepage occurs directly in the refuse with less infiltration when compared to the growth layer. In the uncovered model, the evapotranspiration effect is more evident because of the time reduction for water removal from the model. Two main factors contribute to the covered model evaporation results: i) smaller water content develops lower hydraulic head for water to seep outside the model, and ii) the growth layer as a more porous material retains water.

Table 2. Modeling results summary showing time (days) to return to initial water content

		Precipitation Event			
		1-yr	5-yr	25-yr	100-yr
Steep	Without cover	17	30	50	61
	With cover	25	36	58	63
Flat	Without cover	17	21	29	45
	With cover	26	32	51	66

For visualization of the model response, a time progression of the degree of saturation of the covered steep and flat slopes response for the 25-yr storm was plotted. While similar progression was observed for both steep and flat covered models, there are different saturation levels at day 2 (Figure 8 and 9). The growth layer at the steep model saturates up to 60%; however, the flat model saturates to 70% in the growth layer due to hydraulic head build up. As time progresses, water seeps to the toe of the slope, creating a saturation point (blue area). The crest of the slope desaturates at a faster rate due to evapotranspiration. At day 45, the model returns to similar initial saturation (day 0) conditions. The refuse layer remains with less than 20% saturation throughout time as result of the cover protection. The set water table reflects saturation at the bottom of the model. It remains constant throughout the time steps, not influencing the model behavior.

a) b) c) d) e)

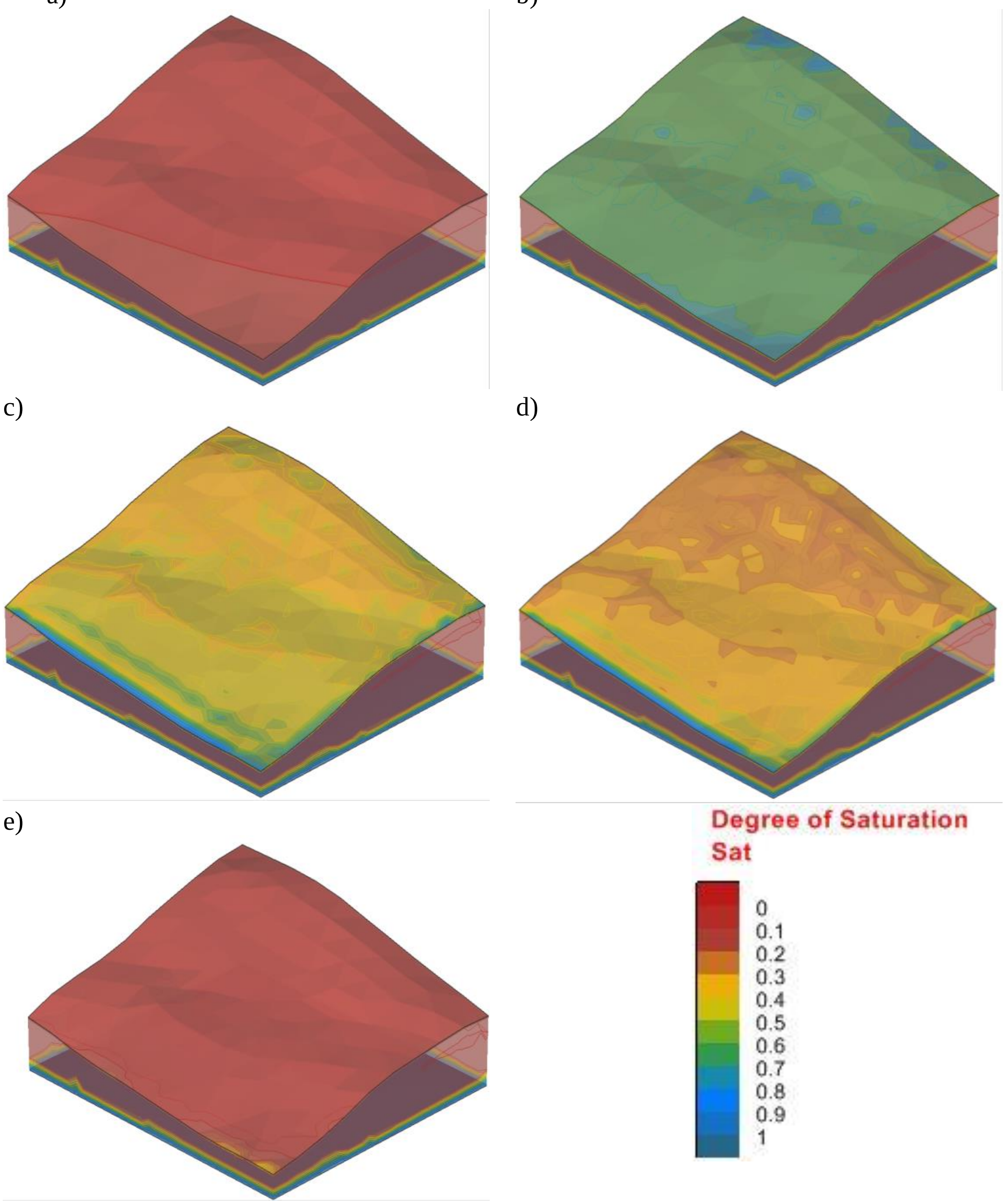

Figure 8. Degree of saturation progression of the covered steep slope model along time due to the 25-yr storm; a) Day 0, b) Day 2, c) Day 10, d) day 15, e) day 45.

The initiation of a drainage channel is present in the center of the flat model. This feature is highlighted at Figure 9 with saturation levels remaining high at the channel (Fig. 9 c and d). The set water table reflects saturation at the bottom of the model. It remains constant throughout the time steps, not influencing the model behavior.

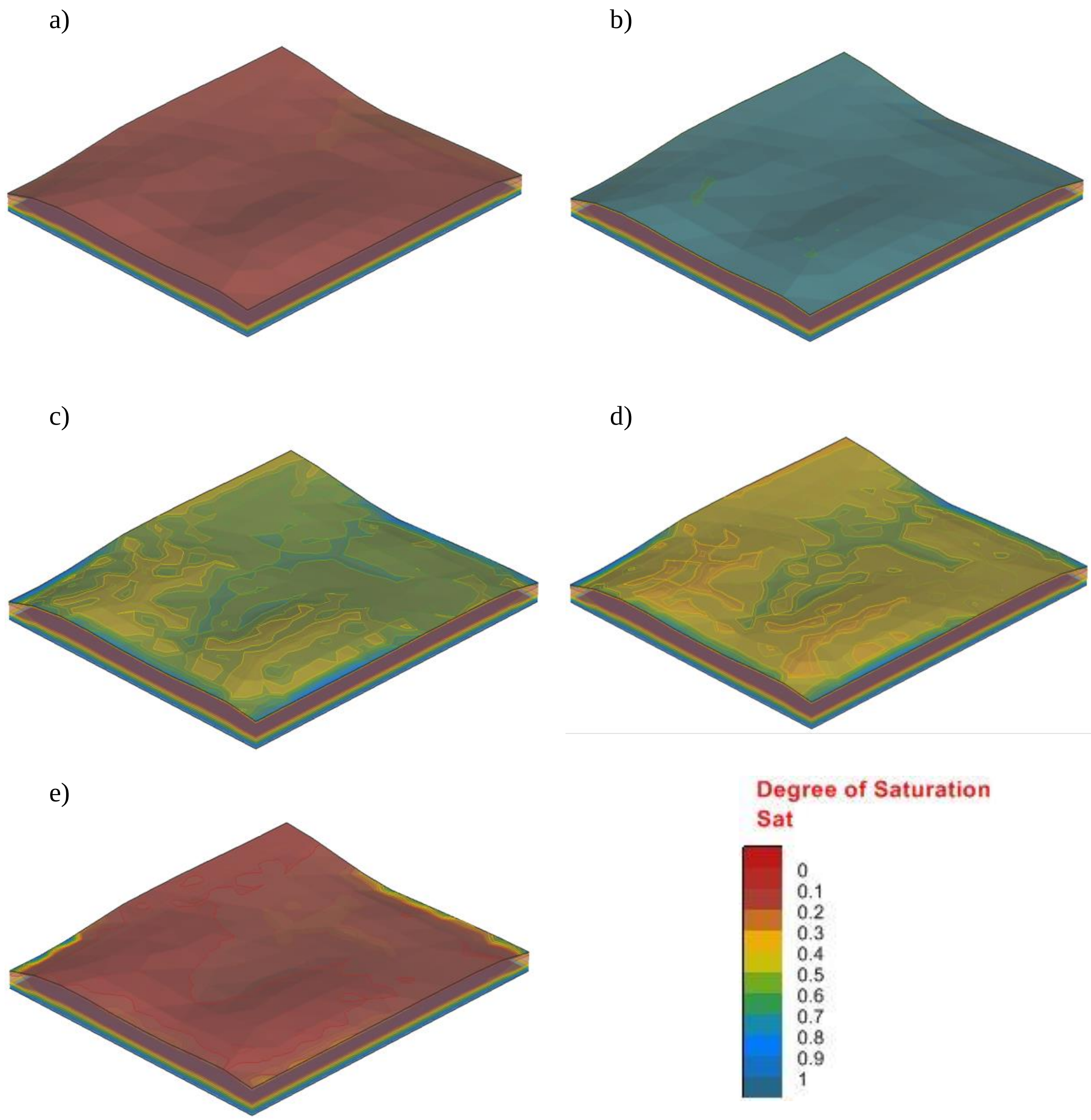

Figure 9. Degree of saturation progression of the covered flat slope model along time due to the 25-yr. storm; a) Day 0, b) Day 2, c) Day 10, d) day 15, e) day 45.

Comparison between the models with the cap and cover system (covered model) and without (uncovered model), indicated that runoff values were larger for the without cap and cover condition, due to the higher porosity of the growth layer. The volumetric increase in runoff follows a similar proportion of precipitation increase, but this pattern is not observed at the covered model. Maximum infiltration to the refuse layer shows a substantial reduction for the covered model (Figure 10 and Figure 11). Maximum water difference at the refuse varies from 50% to 88% for the different storms (Table 3) when compared to the uncovered condition. At the flat uncovered model, runoff decrease at the 100-yr storm compared to the 25-yr due to ponding increasing the hydraulic head. No representative runoff volume was observed with cap and cover model.

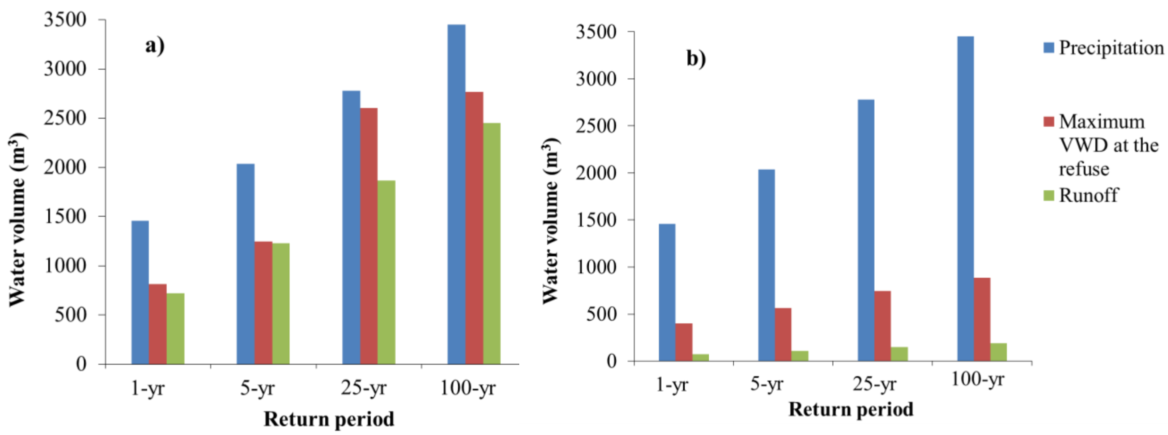

Figure 10. Volumetric water balance analysis comparison at the steep slope model: a) without the cap and cover system and b) with the cap and cover system.

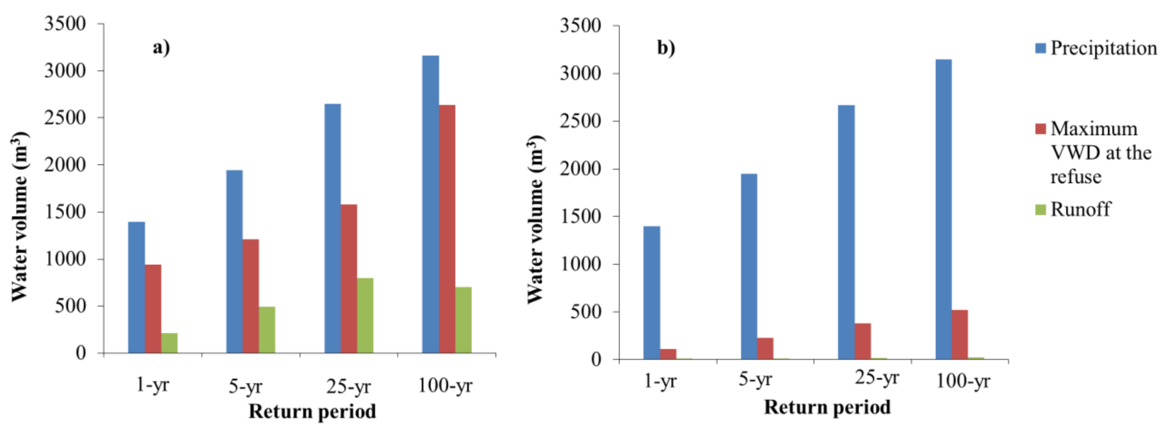

Figure 11. Volumetric water balance analysis comparison at the flat slope model: a) without the cap and cover system and b) with the cap and cover system.

Table 3. Volumetric water difference (%) comparison for the cap and cover system applied to a steep and flat area.

	Precipitation event			
	1-yr	5-yr	25-yr	100-yr
Steep	50	55	71	68
Flat	88	81	76	80

Runoff values are not representative for the without cap and cover models as a result of the model runoff calculation. The model uses indirect pore pressure calculations for runoff volumes resulting in water infiltrating and building the pore pressure downslope in the model, thus water would be infiltrating upslope and raising back downslope, causing double counting in the volume. Minor errors due to the numerical solution nature can be noticed in the results. Comparing the same slope cases, the covered and uncovered models present different precipitation volumes at the 0.001 m^3 order of magnitude.

Growth layer water content

Analysis of the water content in the growth layer can lead to identification of permanent wilting point and field capacity suction based on the pierce model (Harold et al., 1986) contrasting with SWCC of the growth layer (Figure 3). Permanent wilting point (1,500 kPa) is defined as approximately 0.05 volumetric water content; it can be concluded that the water trapped at the growth layer is providing moisture for vegetation. In contrast, field capacity (10 kPa) is at approximately 0.52 volumetric water content (near saturation) and is only reached on days 2 and 3 for the steep slope model and days 2 to 6 for the flat slope model for the 100-yr. storm (Figure 12) event and at days 2 to 4 for the 25-yr storm event.

The growth layer was designed as a loose soil to allow vegetation growth but there is acknowledgment that some compaction will happen due to construction. Moo-Young and Zimmie (1996) studied the properties of short paper fiber residuals and identified that this material naturally consolidates with exposure to environmental conditions, reducing the porosity and consequently decreasing the intrinsic permeability of the soil. Therefore, the runoff over the growth layer is expected to increase, further reducing infiltration. Alternatively, vegetation development will consume near surface water while creating a blockage for evapotranspiration and will act as a physical barrier for sediment transportation.

a)

b)

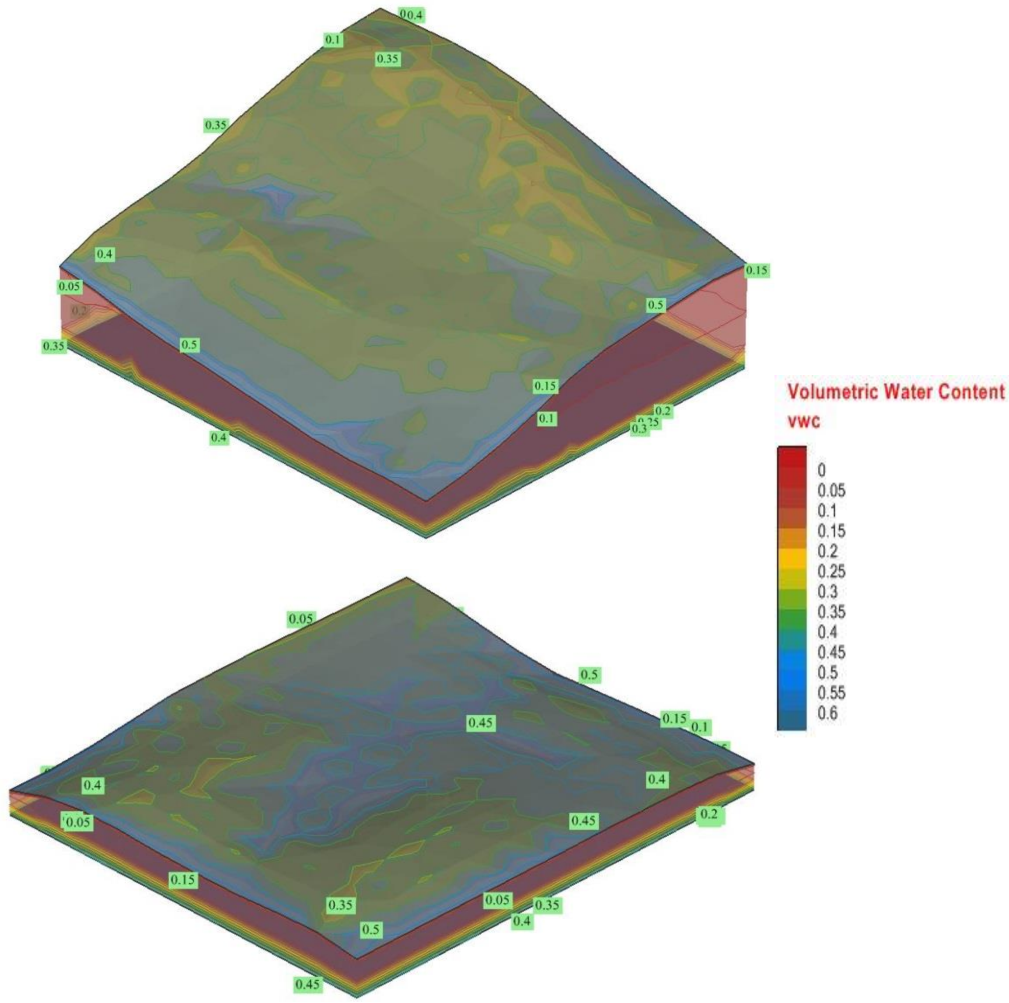

Figure 12. Volumetric water contents responses due to the 100-yr storm: a) steep model at day 3, and b) flat model at day 6.

Relevance and Conclusions

The outcome of this paper is to understand the volumetric difference into the refuse pile due to the implementation of the cap and cover system for different precipitation events. Reduction in infiltration represents cost savings on the AMD treatment by reducing chemical demand, labor, and site maintenance.

The infiltration reduction due to implementation of the barrier varied from of 50% to 88% by the seepage analysis for the tested rainstorm events in two slopes. Effectiveness of the cap and cover system in reducing infiltration is more evident with the flat slopes model as the volume reductions at the refuse were higher than the steep slopes model. Reduction in infiltration for the flat slopes model due to the 1-yr precipitation event was 88% compared to 50% for the steep slopes model, for example. An increase in the time to return to initial volumetric water content conditions affirms the effectiveness of the cap and cover system in delaying and reducing water seepage into the refuse.

Reduction of water infiltration into the refuse layer (AMD producer) by the cap and cover system indicates a beneficial alternative for coal refuse piles reclamation using *in-situ* (coal refuse) and waste materials (biosolids). This can represent significant construction cost savings by reducing borrow material volume and haulage while maintaining acceptable infiltration performance.

When comparing the SWCC of the growth layer and the saturation volumes, it can be inferred that the water retained in the growth layer voids will serve to support vegetation since water content did not reach the permanent wilting point (from SWCC, at 1500 kPa: Volumetric water content = 0.05). Saturation values exceed the field capacity at the immediate days following the 100-yr and 25-yr storms and might present some harm for vegetation in case one of these two extreme events occur. As gravity drives water downslope, vegetation water availability at the toe lasts longer indicating a potential better growth area compared to the slope crest.

The results presented herein are intended to model reduction in infiltration. The volumetric water difference in the refuse layer represents the volume of liquid which will seep and react with the pile forming the AMD to be treated. Reduction in water infiltration in coal refuse piles, represents reduction in AMD treatment costs, including labor, chemicals, and power.

Analyzing the long-term cost benefit, the cost reduction in AMD treatment due to the reclamation benefits will equate to the reclamation construction costs. For an average reduction in VWD of 50% (a result from the 1-yr return period storm) due to the implementation of the cap and cover system compared to cost treatment reported for the year of 2015 (i.e., $173,324), reduction in cost due to the reclamation would be $86,662 per year. When comparing the conventional to the geomorphic reclamation, taking the year of 2015 as the base case, the amount saved in treatment costs would equate the difference in construction cost in an 8-year time span, highlighting the benefit of the geomorphic approach.

The model was designed using local conditions and materials. The implementation of the design principles and aspects may be expanded to several other coal refuse piles in the Appalachian region. Modeling allows site material performance prediction, identification of project limitations, critical water accumulation points, and design flaws consequently avoiding failures and re-construction.

Acknowledgements

The work described in this publication was supported by Grant/Cooperative Agreement Number S15AC20020 from the Office of Surface Mining. Its contents are solely the responsibility of the authors and do not necessarily represent the official views of the OSM. This work is also in collaboration with the West Virginia Department of Environmental protection. The authors would also like to thank Mike Sheehan, Nathan Parks, Dave McCoy, Jason Fox (WVDEP), Mike Richardson (OSM) and Jennifer Hause (WVWRI) for their continued support

Literature Cited

Albright, W., C. Benson, and W. Waugh. (2010). Water balance covers for waste containment: principles and practice. Reston, Virginia: American Society of Civil Engineers.

Benson, C., and C. Bareither. (2012). Designing water balance covers for sustainable waste containment: transitioning the state-of-the-art to state-of-the-practice. Geotechnical Engineering State of the Art and Practice: Keynote lectures from GeoCongress 2012, p. 1-33. Oakland, California: American Society of Civil Engineers.

Camberato, J., B. Gagnon, D. Angers, M. Chantigny, and W. Pan. (2006). Pulp and paper mill by-products as soil amendments and plant nutrient sources. Canadian Journal of Soil Science, 86(4), 641-653. https://doi.org/10.4141/S05-120

Carpenter, A., and I. Fernandez. (2000). Pulp Sludge as a Component in Manufactured Topsoil. Journal of Environmental Quality, 29(2), 387-397. https://doi.org/10.2134/jeq2000.00472425002900020004x

Cyphers, L., L. Hopkinson, and J. Quaranta. (2018). Evaluating short paper fiber as a soil amendment for abandoned mine land reclamation in West Virginia. Proceedings of the West Virginia Academy of Science, 90(2), 1-7.

Daniel, D. (1983). Shallow Land Burial of Low-Level Radioactive Waste. Journal of Geotechnical Engineering, 109(1), 40-55. https://doi.org/10.1061/(ASCE)0733-9410(1983)109:1(40)

Daniels, W., and C. Zipper. (2010). Creation and Management of Productive Minesoils. Virginia Cooperative Extension, 460-121, 1-13.

Fredlund, D., and A. Xing. (1994). Equations for the soil-water characteristic curve. Canadian Geotechnical Journal, 31(3), 521-532. https://doi.org/10.1139/t94-061

Fredlund, D., A. Xing, and S. Huang. (1994). Prediction the permeability function for unsaturated soils using the soil-water characteristic curve. Canadian Geotechnical Journal, 31(4), 533-546. https://doi.org/10.1139/t94-062

Gray, D., and R. Sotir. (1995). Biotechnical stabilization of steepened slopes. Transportation Research Board 746th Annual Meeting, p. 1-17. Washington, District of Columbia: Transportation Research Board.

Harold, L., G. Schwab, and B. Bondurant. (1986). Agricultural and Forest Hydrology. Ohio State University, Agricultural Engineering Department, Columbus, Ohio.

Hernandez, G.T. (2011). Estimating the soil-water characteristic curve using grain size analysis and plasticity index. M.S. Thesis. Tempe, Arizona: Arizona State University.

Hopkinson, L., J. Lorimer, J. Stevens, H. Russel, J. Hause, J. Quaranta, and P. Ziemkiewicz. (2017). Geomorphic landform design principles applied to an abandoned coal refuse pile in central Appalachia. Journal American Society of Mining and Reclamation, 6(2), 19-36. https://doi.org/10.21000/JASMR17020019

Johnson, D., and K. Hallberg. (2005). Acid mine drainage remediation options: A review. Science of the Total Environment, 338(1), 3-14. https://doi.org/10.1016/j.scitotenv.2004.09.002

Kim, H., and C. Benson. (2004). Contributions of advective and diffusive oxygen transport through multilayer composite caps over mine waste. Journal of Contaminant Hydrology, 71, 193-218. https://doi.org/10.1016/j.jconhyd.2003.10.001

Lu, N., and W. Likos. (2014). Unsaturated Soil Mechanics. Hoboken, New Jersey: John Willey and Sons, Inc.

Lunt, H. (1955). The use of woodchips and other wood fragments as soil amendments. New Haven, Connecticut: The Connecticut Agricultural Experiment Station.

Moo-Young, H., and T. Zimmie. (1996). Geotechnical properties of paper mill sludges for use in landfill covers. Journal of Geotechnical Engineering, 122(9), 768-775. https://doi.org/10.1061/(ASCE)0733-9410(1996)122:9(768)

NOAA. (2018). Precipitation Frequency Data Server. https://hdsc.nws.noaa.gov/hdsc/pfds/pfds_map_cont.html?bkmrk=wv , (accessed December 11, 2018)

NREL. (2019). National Renewable Energy Laboratory. https://www.nrel.gov/gis/images/state-level-resource-maps/dni/West-Virginia-DNI-2017-01.jpg . (Accessed January 16, 2019).

Nyhan, J., T. Hakonson, and B. Drennon. (1990). A water balance study of two landfill cover designs for semiarid regions. Journal of Environmental Quality, 19(2), 281-288. https://doi.org/10.2134/jeq1990.00472425001900020014x

Peppas, A., K. Komnitsas, and I. Halikia. (2000). Use of organic covers for acid mine drainage control. Minerals Engineering, 13(5), 563-574. https://doi.org/10.1016/S0892-6875(00)00036-4

Rowe, R., and M. Hosney. (2013). Laboratory investigation of GCL performance for covering arsenic contaminated mine wastes. Geotextile and Geomembranes, 39, 63-77. https://doi.org/10.1016/j.geotexmem.2013.06.003

Santos, I,L. (2017). 3D Finite Element Seepage and Slope Stability Modeling of a Geomorphic Landform Reclamation. M.S. Thesis. Morgantown, West Virginia: West Virginia University.

Schuman, E.M., and T. Sedbrook. (1984). Sawmill wood residue for reclaiming bentonite spoils. Forest Products Journal, 34, 65-68.

Seaker, E., and W. Sopper. (1983). Reclamation of deep mine refuse banks with municipal sewage sludge. Waste Management & Research, 1(4), 309-322. https://doi.org/10.1016/0734-242X(83)90035-6

Skousen, J., and C. Clinger. (1993). Sewage sludge land application program in West Virginia. Journal of Soil and Water Conservation, 48(2), 145-151.

Skousen, J., P.F. Ziemkiewicz, and L.M. McDonald. (2019). Acid mine drainage formation, control and treatment: Approaches and Strategies. The Extractive Industries and Society, 6, 241-249. https://doi.org/10.1016/j.exis.2018.09.008

Stevens, J. (2016). Geotechnical testing and finite element modeling of geomorphic landform design with a multi-layer cap and cover system. M.S. Thesis. Morgantown, West Virginia: West Virginia University.

Tolikonda, R. (2010). Nonwoven geotextile filtration performance with coal refuse. M.S. Thesis. Morgantown, West Virginia, USA: West Virginia University.

Ward, K. (2001). A toxic legacy. Charleston Gazette-Mail. www.wvgazettemail.com/News/MiningtheMountains/200108120003 (accessed August 17, 2018)

Warren, R., T. Hakonson, and K. Bostick. (1996). Choosing the most effective hazardous waste landfill cover. The Journal of Environmental Cleanups Costs Technologies and Techniques, 6(2), 23-41. https://doi.org/10.1002/rem.3440060205

Wilson, G., D. Fredlund, and S. Barbour. (1994). Coupled soil-atmosphere modelling for soil evaporation. Canadian Geotechnical Journal, 31, 151-161. https://doi.org/10.1139/t94-021

Zapata, C. (1999). Soil-water characteristic curve and impacts on unsaturated shear strength predictions. Ph.D. Dissertation. Tempe, Arizona: Arizona State University.

Ziadi, N., B. Gagnon, J. Nyiraneza. (2013) Crop yield and soil fertility as affected by papermill biosolids and liming by-products. Canadian Journal of Soil Science, 93(3), 319-328. https://doi.org/10.4141/cjss2012-129